External Review on Center for Computational Sciences
University of Tsukuba
2013.2.18-20

Time-Dependent Density Functional Theory in Optical Sciences

K. YABANA

Center for Computational Sciences, University of Tsukuba

Collaborators:

G.F. Bertsch	Univ. Washington
T. Otobe	JAEA
J.-I. Iwata	Univ. Tokyo
S. Shinohara	Univ. Tsukuba/MPI
T. Sugiyama	Univ. Tsukuba
S.A. Sato	Univ. Tsukuba

First-principles electron dynamics simulation based on Time-Dependent Density Functional Theory (TDDFT)

Real-time and real-space solution of time-dependent Kohn-Sham equation

$$\left\{-\frac{\hbar^2}{2m}\vec{\nabla}^2+\sum_a V_{ion}(\vec{r}-\vec{R}_a)+e^2\int d\vec{r}'\frac{n(\vec{r}',t)}{|\vec{r}-\vec{r}'|}+\mu_{xc}(n(\vec{r},t))+V_{ext}(\vec{r},t)\right\}\psi_i(\vec{r},t)=i\hbar\frac{\partial}{\partial t}\psi_i(\vec{r},t)$$

$$n(\vec{r},t)=\sum_i|\psi_i(\vec{r},t)|^2$$

Development of methodology and our own softwear
ARTED = Ab-initio Real-Time Electron Dynamics simulator

1996 Isolated system (molecules, clusters)
K. Yabana, G.F. Bertsch,
Phys. Rev. B54, 4484 (1996).

2000 Infinitely periodic system (crystalline solids)
G.F. Bertsch, J.-I. Iwata, A. Rubio, K. Yabana,
Phys. Rev. B62, 7998 (2000).

2012 Coupling to macroscopic Maxwell equation
K. Yabana, T. Sugiyama, Y. Shinohara, T. Otobe, G.F. Bertsch,
Phys. Rev. B85, 045134 (2012).

$\psi_m(x_i, y_j, z_k, t_l)$

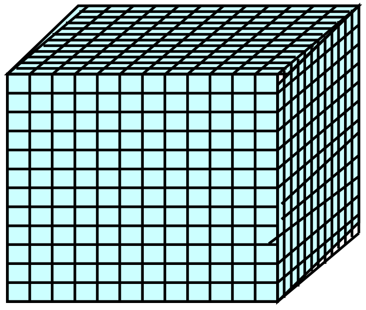

2008 - 2013

Linear optical absorption in molecules

K. Yabana, Y. Kawashita, T. Nakatsukasa, J.-I. Iwata,
Charged Particle and Photon Interactions with Matter:
Recent Advances, Applications, and Interfaces Chapter 4, Taylor & Francis, 2010.

Electron dynamics in crystalline solids under femtosecond laser pulses

- Optical breakdown of dielectrics

T. Otobe, M. Yamagiwa, J.-I. Iwata, K. Yabana, T. Nakatsukasa, G.F. Bertsch
Phys. Rev. B77, 165104 (2008).

- Coherent phonon generation

Y. Shinohara, K. Yabana, Y. Kawashita, J.-I. Iwata, T. Otobe, G.F. Bertsch
Phys. Rev. B82, 155110 (2010)
Y. Shinohara, S.A. Sato, K. Yabana, J.-I. Iwata, T. Otobe, G.F. Bertsch
J. Chem. Phys. 137, 22A527 (2012).

Coupled dynamics of macroscopic electromagnetic fields and microscopic electron dynamics

K. Yabana, T. Sugiyama, Y. Shinohara, T. Otobe, G.F. Bertsch
Phys. Rev. B85, 045134 (2012).

2008 - 2013

Linear optical absorption in molecules

K. Yabana, Y. Kawashita, T. Nakatsukasa, J.-I. Iwata,
Charged Particle and Photon Interactions with Matter:
Recent Advances, Applications, and Interfaces Chapter 4, Taylor & Francis, 2010.

Electron dynamics in crystalline solids under femtosecond laser pulses

- Optical breakdown of dielectrics

T. Otobe, M. Yamagiwa, J.-I. Iwata, K. Yabana, T. Nakatsukasa, G.F. Bertsch
Phys. Rev. B77, 165104 (2008).

- Coherent phonon generation

Y. Shinohara, K. Yabana, Y. Kawashita, J.-I. Iwata, T. Otobe, G.F. Bertsch
Phys. Rev. B82, 155110 (2010)
Y. Shinohara, S.A. Sato, K. Yabana, J.-I. Iwata, T. Otobe, G.F. Bertsch
J. Chem. Phys. 137, 22A527 (2012).

Coupled dynamics of macroscopic electromagnetic fields and microscopic electron dynamics

K. Yabana, T. Sugiyama, Y. Shinohara, T. Otobe, G.F. Bertsch
Phys. Rev. B85, 045134 (2012).

Working in two fields
Nuclear Physics and Condensed Matter Physics
has brought us original developments

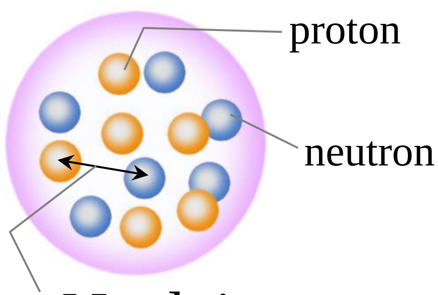

Nuclei

Nucleon many-body system

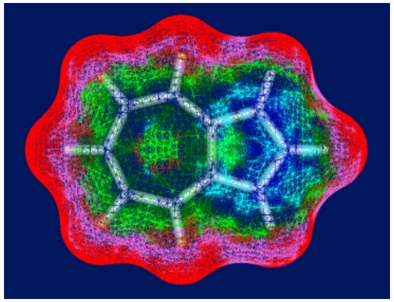

Atoms, Molecules, Solids

Electron many-body systems

Common theories and computational methods are useful.

In nuclear physics, 3D simulation solving TDHF eq. has long history.

One of the oldest 3D quantum-mechanical simulation

Nuclear fusion reaction of ^{16}O-^{16}O

Spatial grid: 30x28x16 (10^{-15}m), Time-step 4×10^{2} (10^{-22}s)

17 H. Flocard, S.E. Koonin, M.S. Weiss, Phys. Rev. 17(1978)1682.

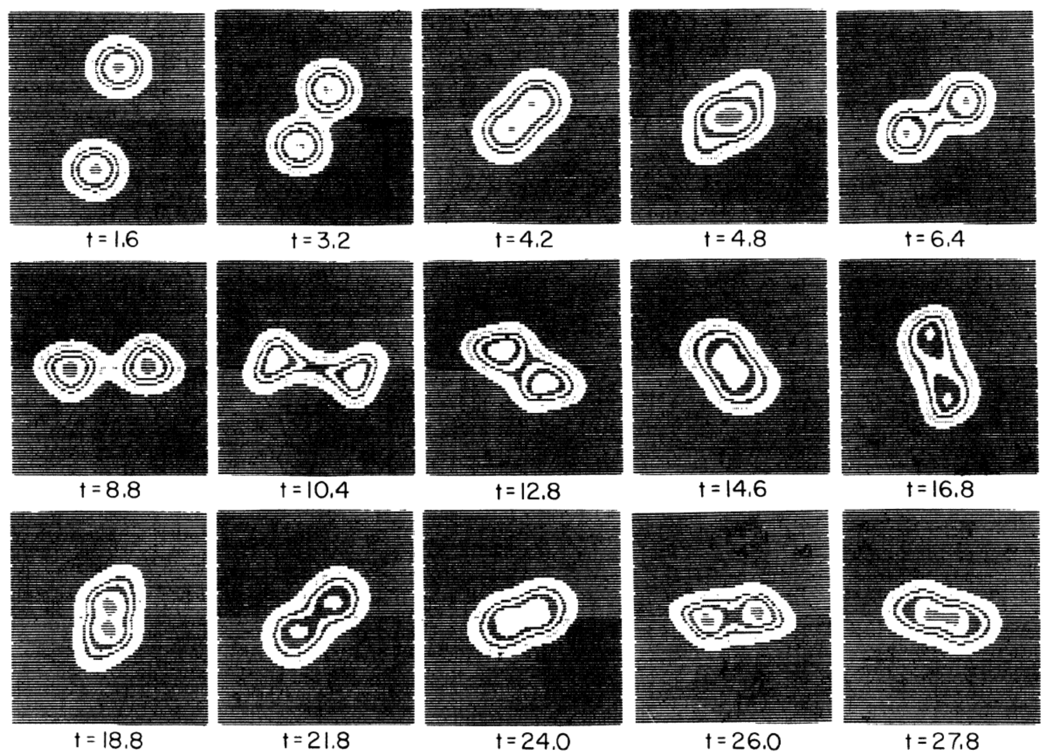

FIG. 2. Contour lines of the density integrated over the coordinate normal to the scattering plane for an $^{16}O + ^{16}O$ collision at $E_{lab} = 105$ MeV and incident angular momentum $L = 13\hbar$. The times t are given in units of 10^{-22} sec.

Electron dynamics in metallic clusters by TDDFT

K. Yabana, G.F. Bertsch, Phys. Rev. B54, 4484 (1996).

Assume
Icosahedral shape

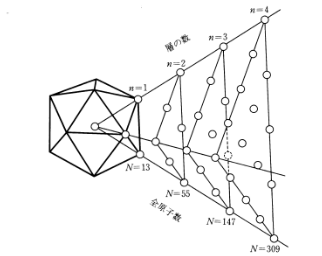

図 5·61 多層正二十面体構造(MIC)の概念図[104]
n は MIC の層の数であり，N は全原子数である。1 層構造($n=1$)では原子数 $N=13$ に対応し，2 層構造($n=2$)では $N=55$，3 層構造($n=3$)では $N=147$…となる。

Li_{147}^{+}

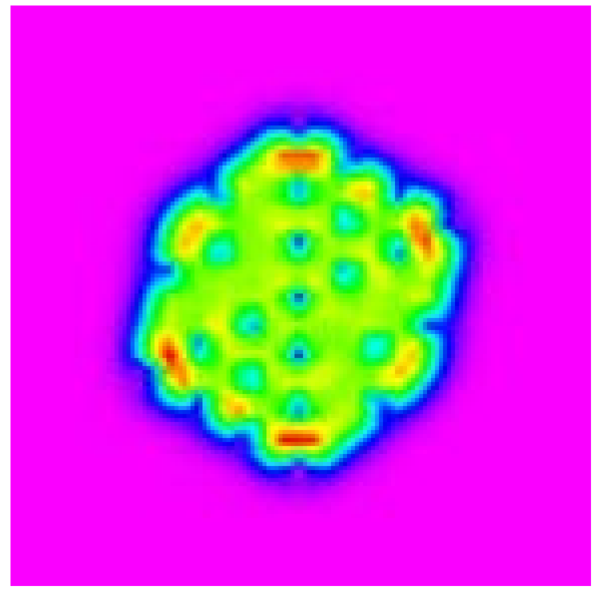

Density change induced by impulsive force

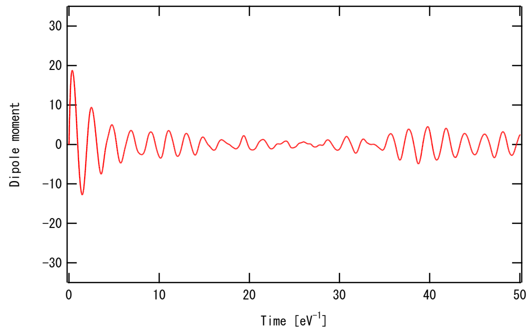

Dipole moment as function of time

Real-time calculation for optical absorption spectrum of Li_{147}^{+}

K. Yabana, G.F. Bertsch, Phys. Rev. B54, 4484 (1996).

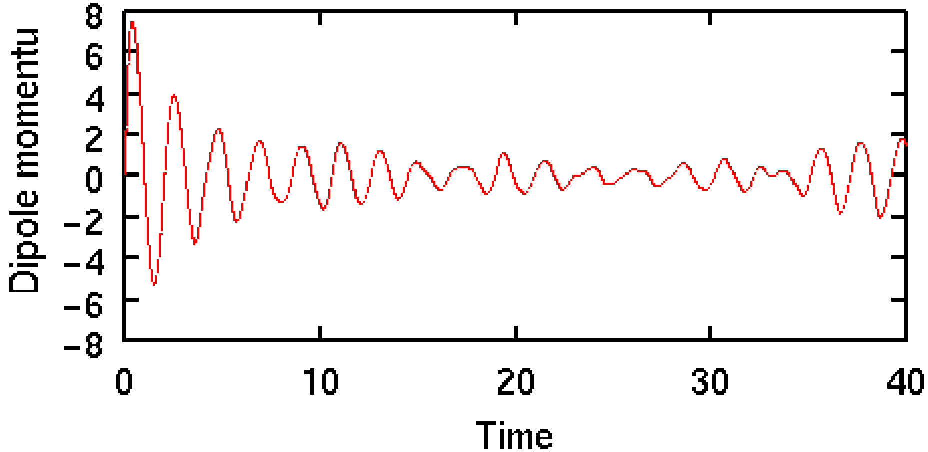

Real-time calculation
for autocorrelation function

$$\langle \hat{z}(t)\hat{z}(0)\rangle$$

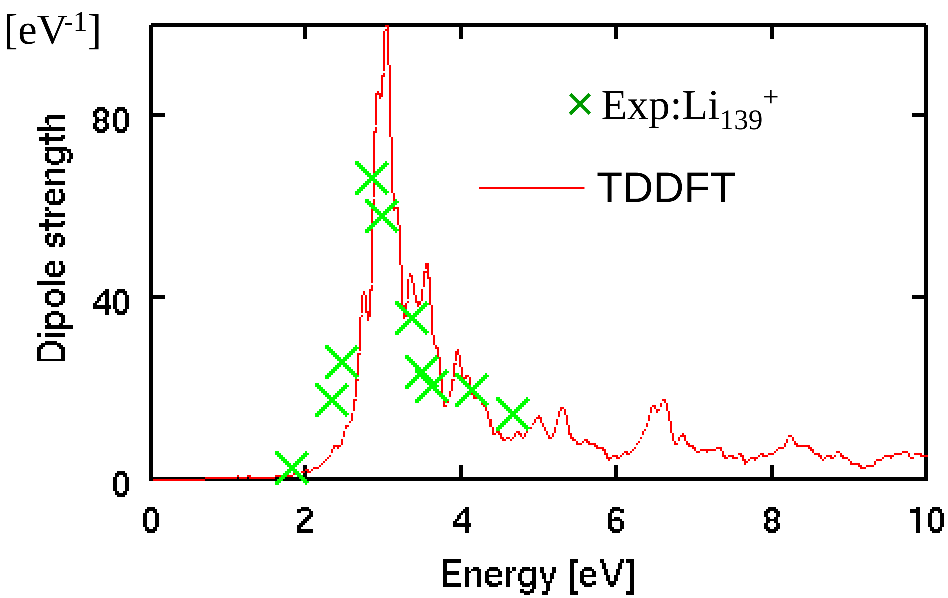

Fourier transformation
→ oscillator strength distribution

$$\sigma(\omega) \propto \frac{1}{k}\int dt\, e^{i\omega t}\langle \hat{z}(t)\hat{z}(0)\rangle$$

Photoabsorption of molecules by TDDFT (LB94 functional)

"Continuum RPA calculation for deformed system"

K. Yabana, Y. Kawashita, T. Nakatsukasa, J.-I. Iwata, Charged Particle and Photon Interactions with Matter: Recent Advances, Applications, and Interfaces Chapter 4, Taylor & Francis, 2010.

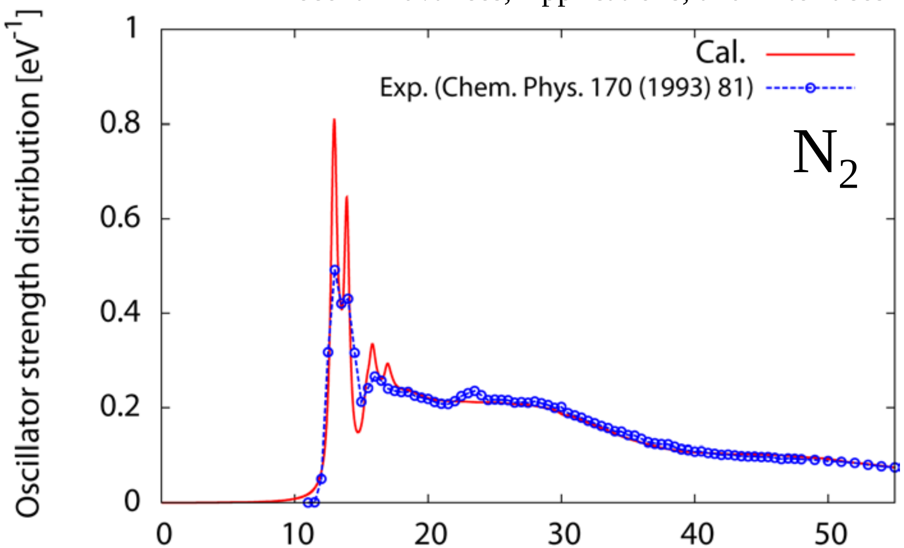

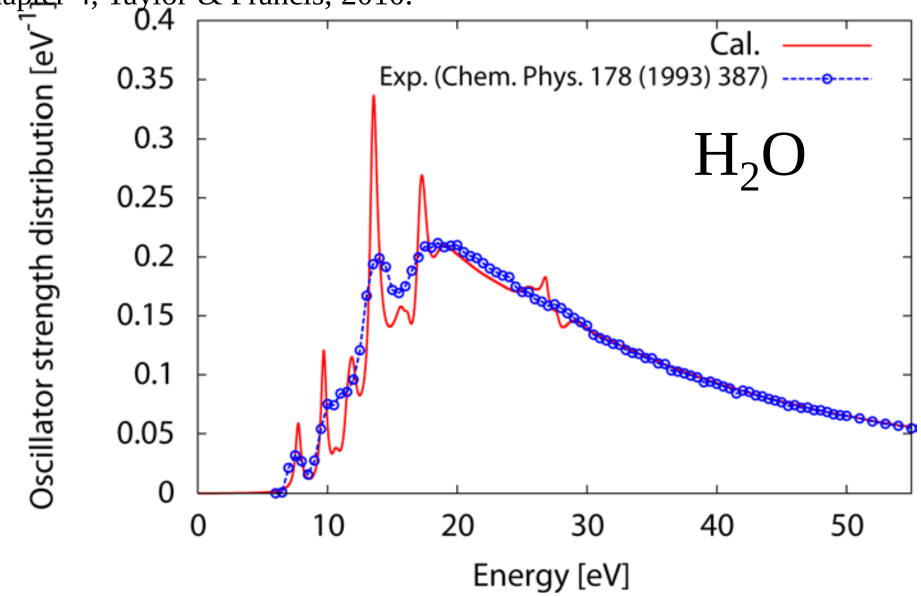

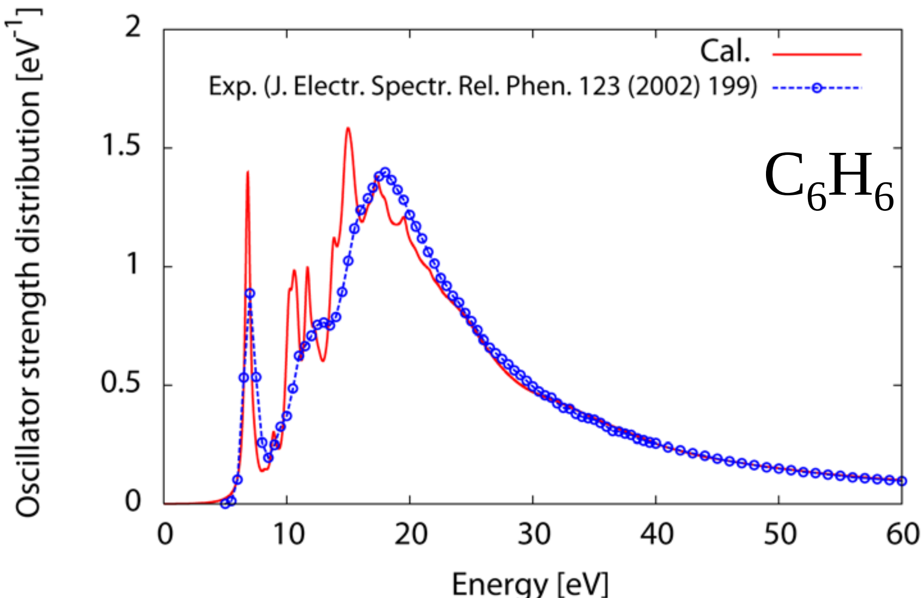

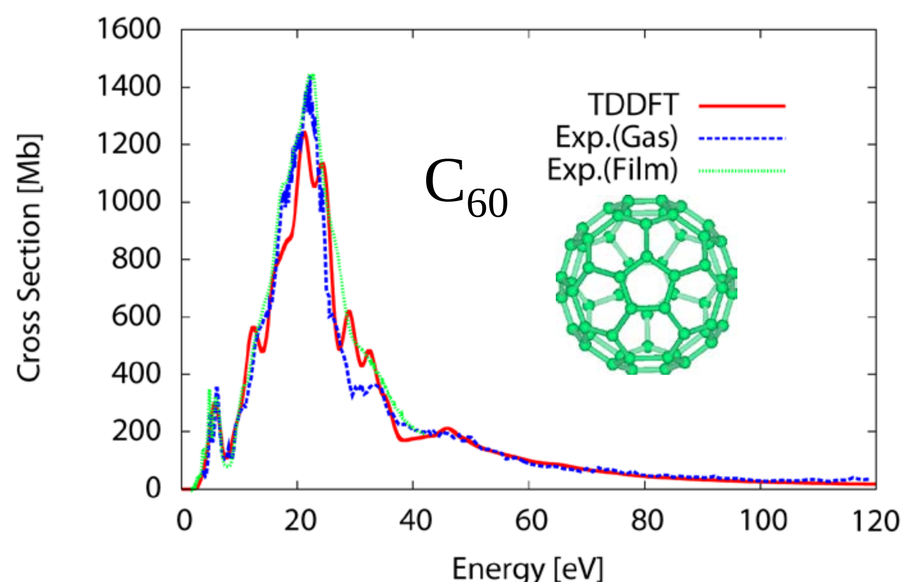

2008 - 2013

Linear optical absorption in molecules

K. Yabana, Y. Kawashita, T. Nakatsukasa, J.-I. Iwata,
Charged Particle and Photon Interactions with Matter:
Recent Advances, Applications, and Interfaces Chapter 4, Taylor & Francis, 2010.

Electron dynamics in crystalline solids under femtosecond laser pulses

- Optical breakdown of dielectrics

T. Otobe, M. Yamagiwa, J.-I. Iwata, K. Yabana, T. Nakatsukasa, G.F. Bertsch
Phys. Rev. B77, 165104 (2008).

- Coherent phonon generation

Y. Shinohara, K. Yabana, Y. Kawashita, J.-I. Iwata, T. Otobe, G.F. Bertsch
Phys. Rev. B82, 155110 (2010)
Y. Shinohara, S.A. Sato, K. Yabana, J.-I. Iwata, T. Otobe, G.F. Bertsch
J. Chem. Phys. 137, 22A527 (2012).

Coupled dynamics of macroscopic electromagnetic fields and microscopic electron dynamics

K. Yabana, T. Sugiyama, Y. Shinohara, T. Otobe, G.F. Bertsch
Phys. Rev. B85, 045134 (2012).

Time-dependent extension of Bloch's band theory

$$i\hbar \frac{\partial}{\partial t} u_{n\vec{k}}(\vec{r},t) = \left[\frac{1}{2m}\left(\vec{p} + \vec{k} + \frac{e}{c}\vec{A}(t) \right)^2 + \int d\vec{r}\,' \frac{e^2}{|\vec{r}-\vec{r}\,'|} n(\vec{r}\,',t) + \mu_{xc}[n(\vec{r},t)] \right] u_{n\vec{k}}(\vec{r},t)$$

$$n(\vec{r},t) = \sum_{nk} \left| u_{n\vec{k}}(\vec{r},t) \right|^2$$

$$u_{nk}(\vec{r}+\vec{a},t) = u_{nk}(\vec{r},t)$$

Electron dynamics in crystalline solid (atomic positions are fixed)

Computational aspects
- 3D uniform gird for space, high-order finite difference for differentiation
- Taylor expansion for time evolution

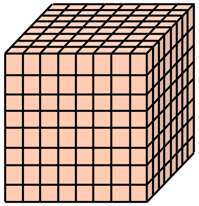

Electron dynamics in bulk Si under strong laser pulse

I= 3.5×10^{14} W/cm^2, T=50 fs, $\hbar\omega$=0.5 eV

Laser photon energy is much lower than direct bandgap.

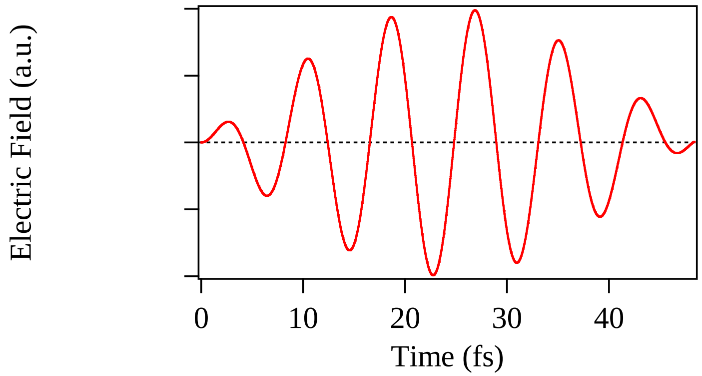

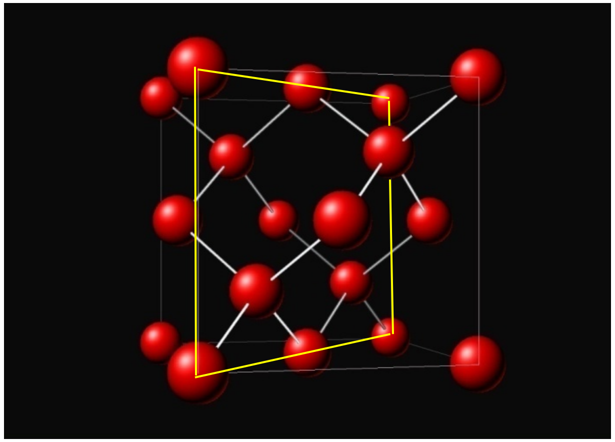

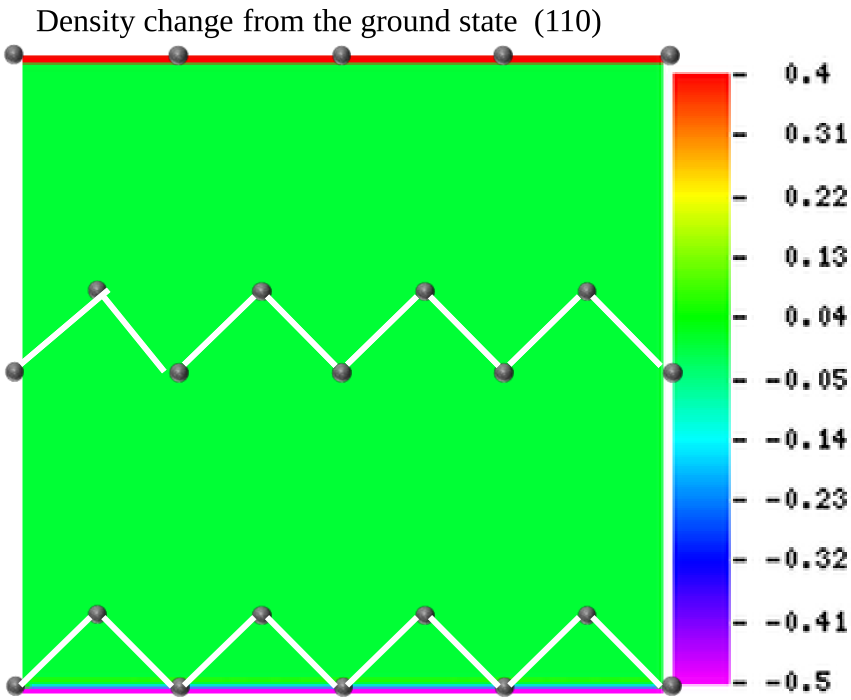

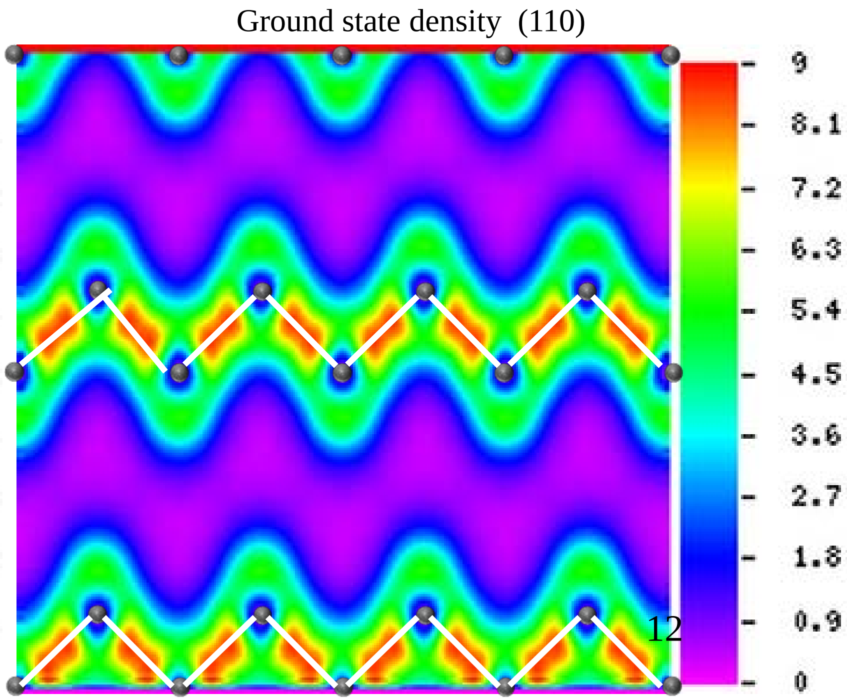

Red +
Green 0
Blue -

Dielectric function of Si from real-time TDDFT-ALDA

Instantaneous kick at t=0, then calculate current *J(t)*

$$\sigma(\omega) = \frac{1}{k}\int dt\, e^{i\omega t} J(t), \quad \varepsilon(\omega) = 1 + \frac{4\pi i \sigma(\omega)}{\omega}$$

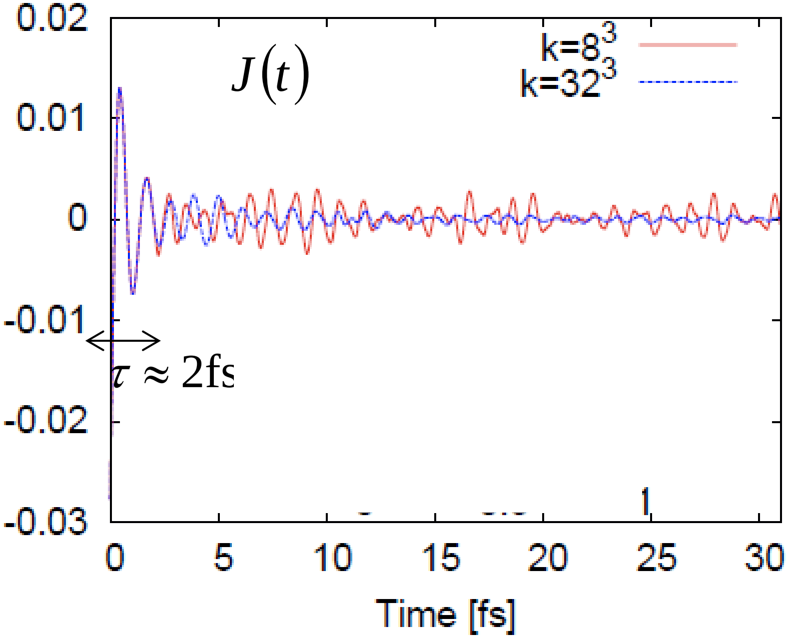

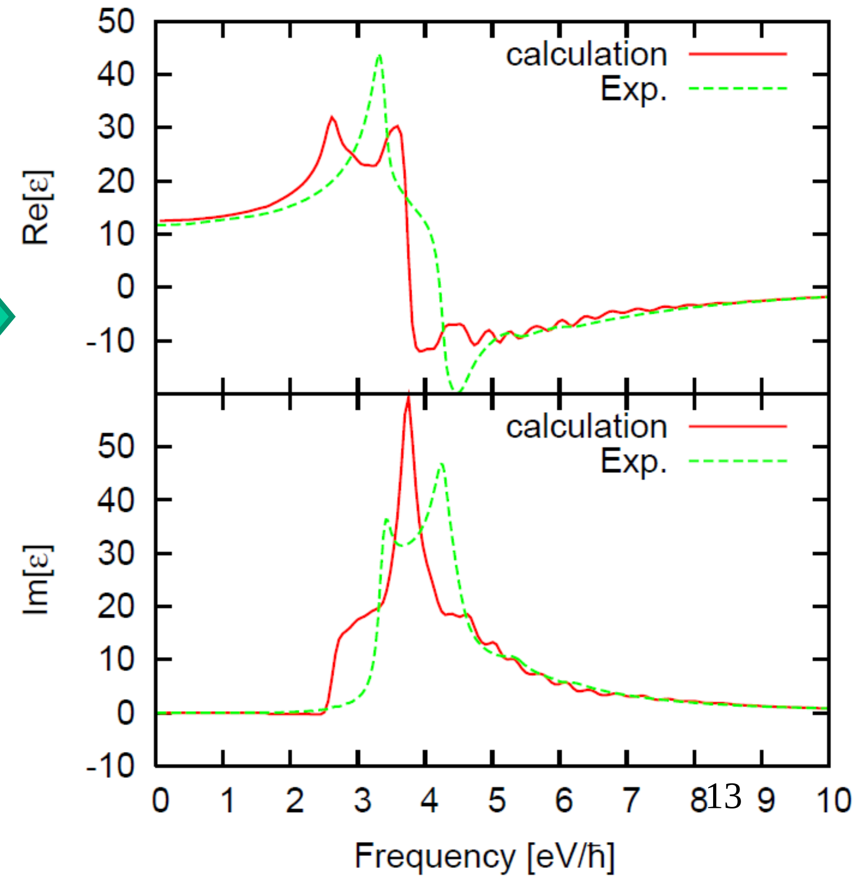

Not very good in quality.

Intense and ultrashort laser pulse on Si: Multi-photon to tunnel/field ionizations

$\hbar\omega = 1.55\mathrm{eV}$

$(\text{direct bandgap } 2.4\,\mathrm{eV} \text{ in LDA})$

$I = 3.2\times10^{12}\,\mathrm{W/cm^2}$

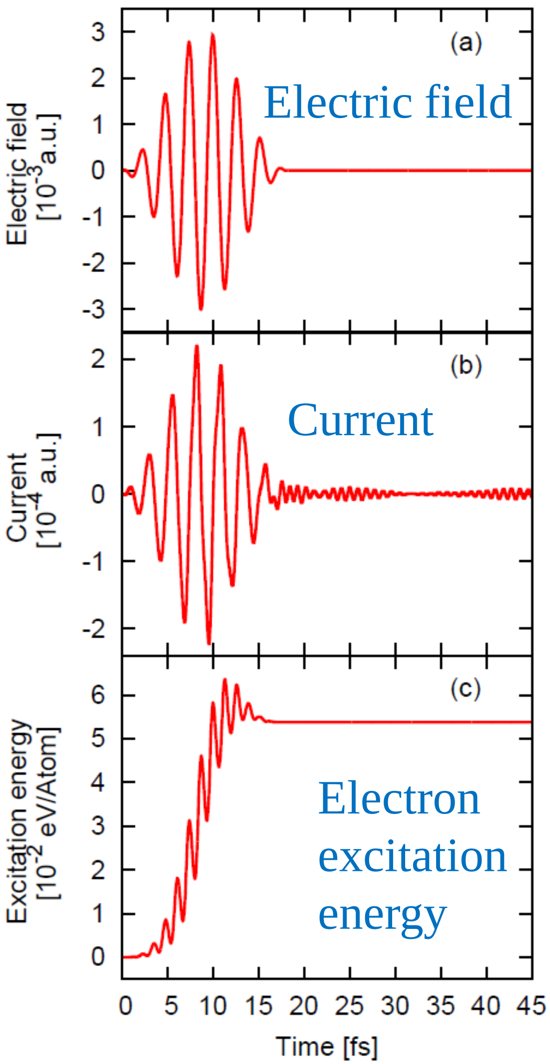

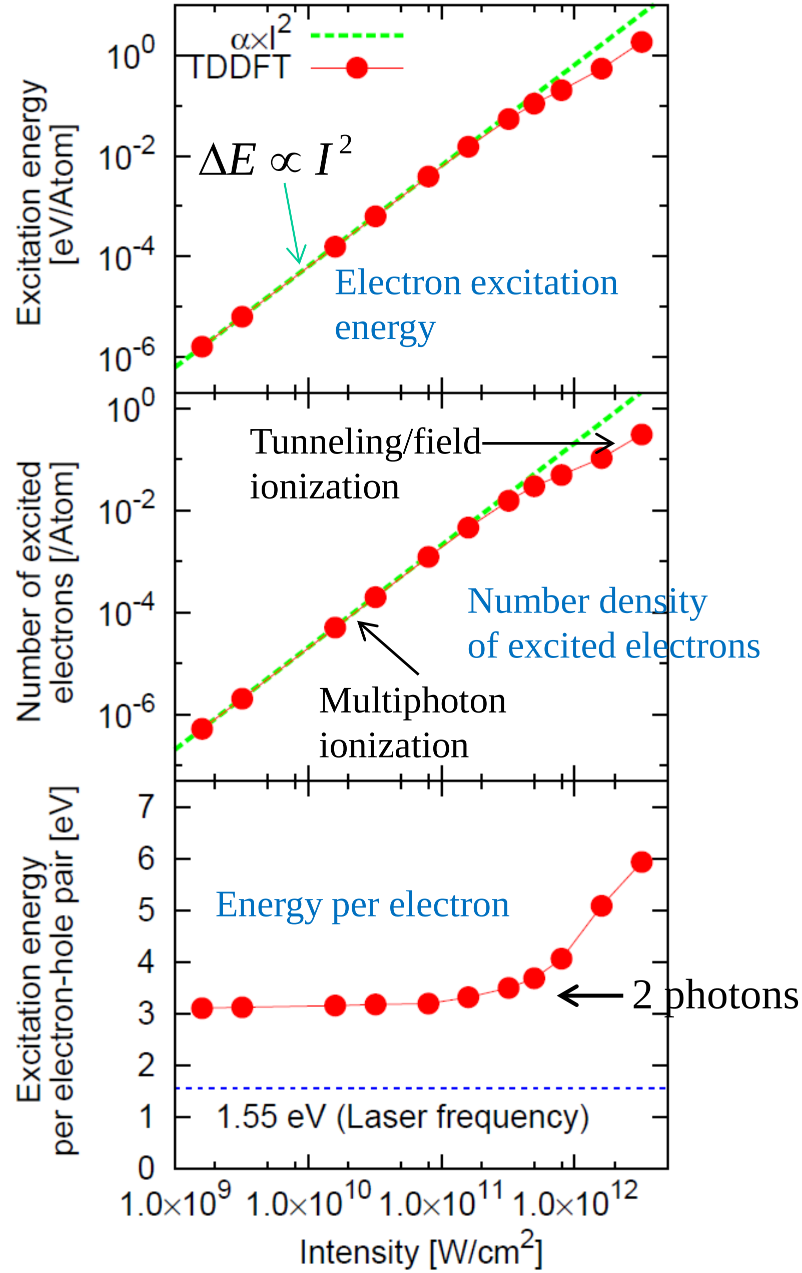

Laser-Matter interaction: Strong and Ultra-Short Laser Pulse

Strong light field

Magnitude of light electric field comparable to that bound electrons in matters.

Nonlinear, nonequilibrium
Electron Dynamics

Ultra-short pulse

Pulse time duration comparable to a period of electron motion in matters.

Femto-technology
Atto-second science

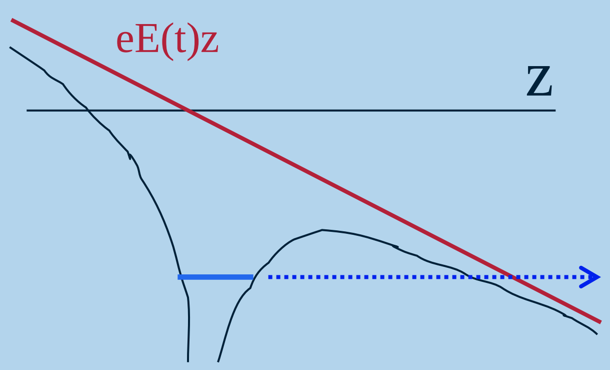

Real-time observation of laser electric field using atto-second streaking technique

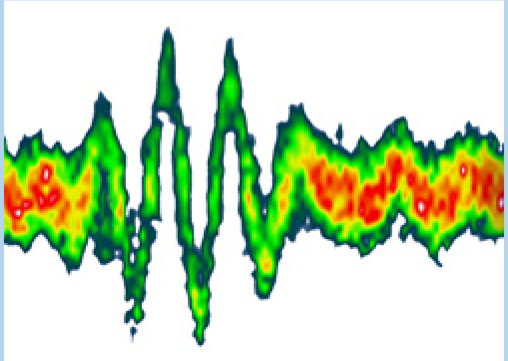

Joint LMU-MPQ Laboratory of Attosecond

Nonthermal Laser Machinery

Melting, ablation, filamentation on bulk surface

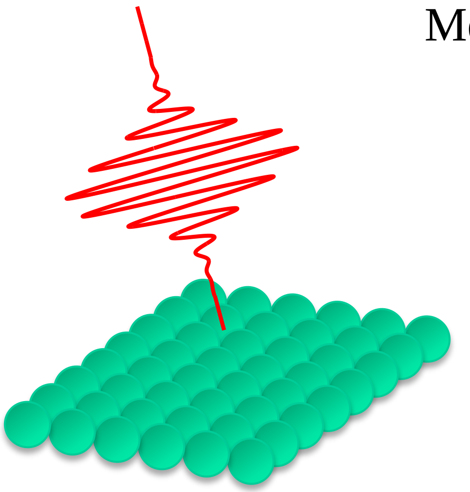

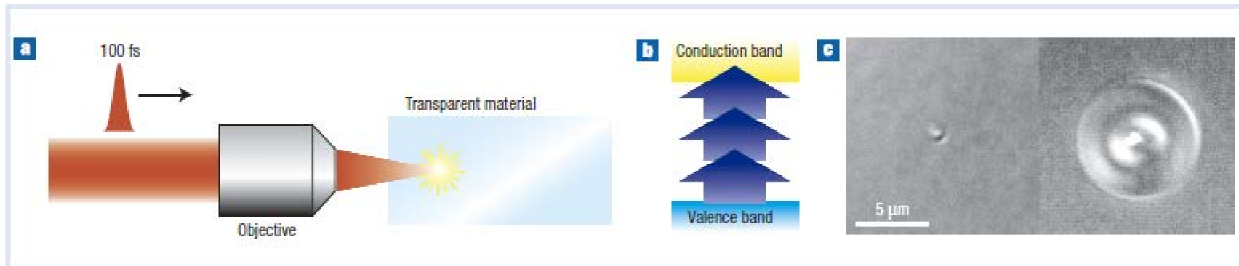

Figure B1 Femtosecond laser micromaching process. **a**, Schematic of the laser incident on a transparent material. **b**, Diagram of the excitation of electrons to the conduction band. **c**, Microscope images showing the large variation in the feature characteristics depending on the experimental conditions. Left: single 10-nJ pulse and right: 25,000 5-nJ pulses at a frequency of 25 MHz (both with the same focal spot).

R.R. Gattass, E. Mazur, Nature Photonics 2, 220 (2008).

Micromachining – waveguide-

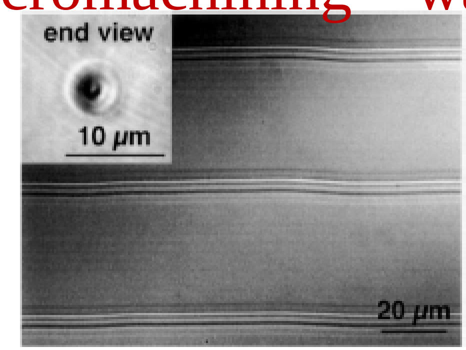

Optical microscope image of waveguides written inside bulk glass by a 25-MHz train of 5-nJ sub-100-fs pulses, C.B. Schaffer et.al, OPTICS LETTERS 26, 93 (2001)

Nanosurgery

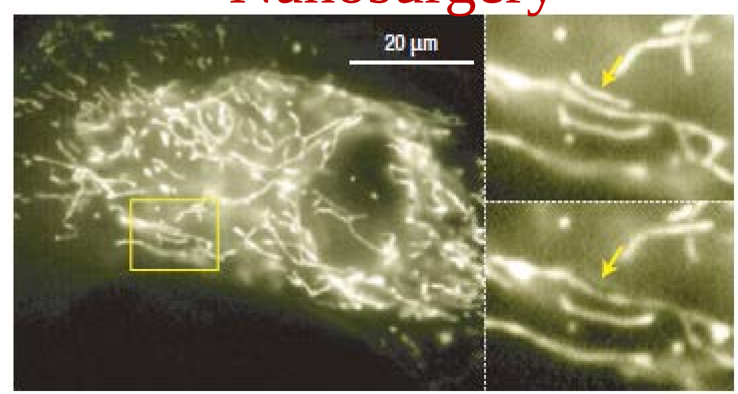

Ablation of a single mitochondrion in a living cell.
N. Shen et.al, Mech. Chem. Biosystems, 2, 17 (2005).

2008 - 2013

Linear optical absorption in molecules

K. Yabana, Y. Kawashita, T. Nakatsukasa, J.-I. Iwata,
Charged Particle and Photon Interactions with Matter:
Recent Advances, Applications, and Interfaces Chapter 4, Taylor & Francis, 2010.

Electron dynamics in crystalline solids under femtosecond laser pulses

- Optical breakdown of dielectrics

T. Otobe, M. Yamagiwa, J.-I. Iwata, K. Yabana, T. Nakatsukasa, G.F. Bertsch
Phys. Rev. B77, 165104 (2008).

- Coherent phonon generation

Y. Shinohara, K. Yabana, Y. Kawashita, J.-I. Iwata, T. Otobe, G.F. Bertsch
Phys. Rev. B82, 155110 (2010)
Y. Shinohara, S.A. Sato, K. Yabana, J.-I. Iwata, T. Otobe, G.F. Bertsch
J. Chem. Phys. 137, 22A527 (2012).

Coupled dynamics of macroscopic electromagnetic fields and microscopic electron dynamics

K. Yabana, T. Sugiyama, Y. Shinohara, T. Otobe, G.F. Bertsch
Phys. Rev. B85, 045134 (2012).

Ordinary macroscopic electromagnetism

Electromagnetism:
Maxwell equation for macroscopic fields,
E, D, B, H

Linear constitutive relation

$$D = D[E] = \varepsilon(\omega)E$$

Quantum Mechanics:
Perturbation theory to calculate linear susceptibilities,
$\varepsilon(\omega)$

As the field strength becomes large,
"nonlinear optics" becomes important.

$$D_\alpha(\vec{r},t) = \int^t dt' \varepsilon_{\alpha\beta}(t-t')E_\beta(\vec{r},t') + 4\pi\int^t dt'\int^t dt'' \chi_{\alpha\beta\gamma}{}^{(2)}(t-t',t-t'')E_\beta(\vec{r},t')E_\gamma(\vec{r},t'') + \cdots$$

At extreme intense limit, EM and QM no more separate.

Coupled dynamics of macroscopic electromagnetic fields and microscopic electron dynamics

K. Yabana, T. Sugiyama, Y. Shinohara, T. Otobe, G.F. Bertsch, Phys. Rev. B85, 045134 (2012).

Multiscale simulation

K. Yabana, T. Sugiyama, Y. Shinohara, T. Otobe, G.F. Bertsch, Phys. Rev. B85, 045134 (2012).

At each macroscopic grid point,
We consider a unit cell and prepare microscopic grid.

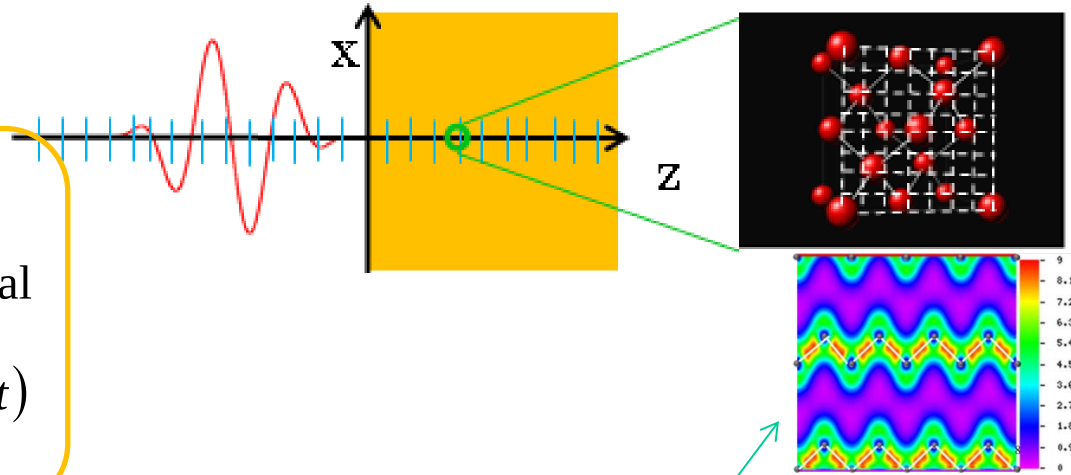

Macroscopic grid points (μm)
to describe macroscopic vector potential

$$\frac{1}{c^2}\frac{\partial^2}{\partial t^2}A(Z,t)-\frac{\partial^2}{\partial Z^2}A(Z,t)=\frac{4\pi}{c}J(Z,t)$$

$J(Z,t)$

Exchange of information by
macroscopic current and
macroscopic vector potential.

$A(Z,t)$

At each macroscopic points, Kohn-Sham orbitals $\psi_{i,Z}$ are prepared, and described in microscopic grids.

$$i\hbar\frac{\partial}{\partial t}\psi_{i,Z}=\frac{1}{2m}\left(-i\hbar\vec{\nabla}+\frac{e}{c}\vec{A}\right)^2\psi_{i,Z}-e\phi_Z\psi_{i,Z}+\frac{\delta E_{xc}}{\delta n}\psi_{i,Z}$$

$$\vec{\nabla}^2\phi_Z=-4\pi\left\{en_{ion}-en_{e,Z}\right\}$$

$$J(Z,t)=\int_\Omega d\vec{r}\,\vec{j}_{e,Z}$$

$$\vec{j}_{e,Z}=\frac{\hbar}{2mi}\sum_i\left(\psi^*_{i,Z}\vec{\nabla}\psi_{i,Z}-\psi_{i,Z}\vec{\nabla}\psi^*_{i,Z}\right)-\frac{e}{4\pi c}n_{e,Z}\vec{A}$$

Propagation of weak pulse

Ordinary electromagnetism is OK.

$I=10^{10}$W/cm^2

Laser frequency：1.55eV：
lower than direct bandgap
2.4eV(LDA)

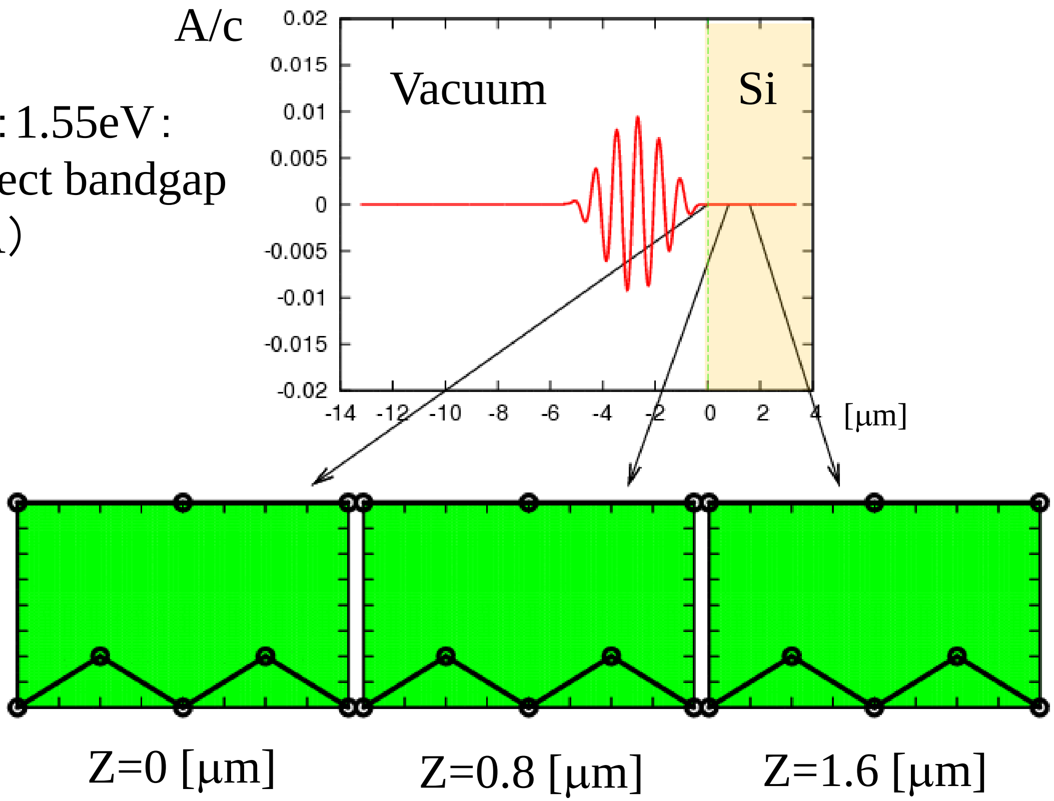

Coupled Maxwell + TDDFT simulation

More intense laser pulse

Dynamics of electrons and macroscopic EM fields are no more separable.

$I = 5 \times 10^{12} W/cm^2$

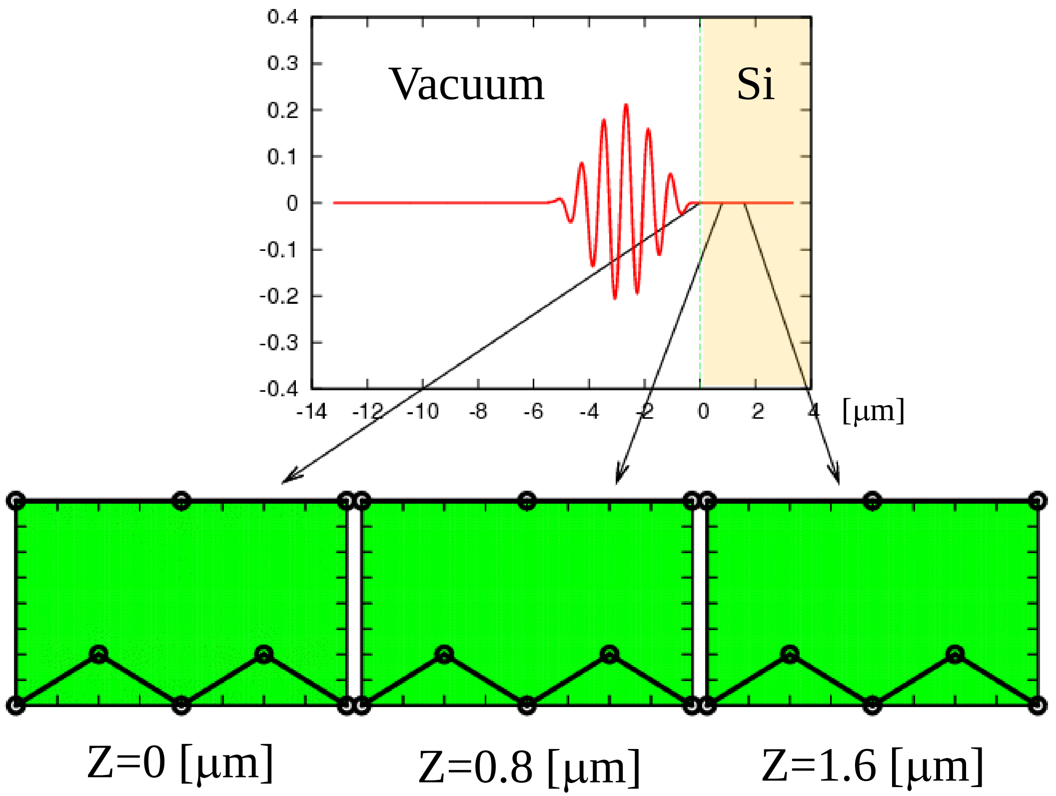

Computationally scalable simulation

1,000 cores, 10 hours
30,000 cores, 20 min (K-computer, Kobe)

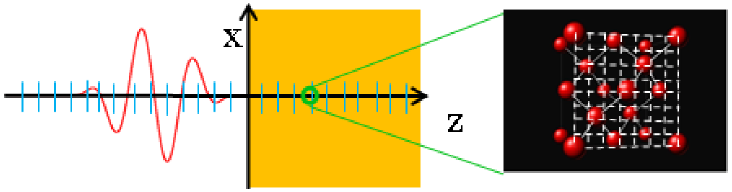

Performance at K-Computer in Kobe (in early access)

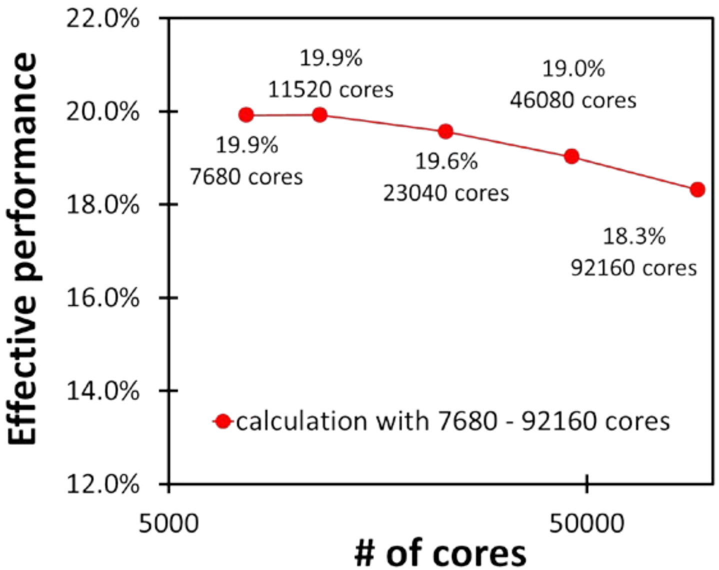

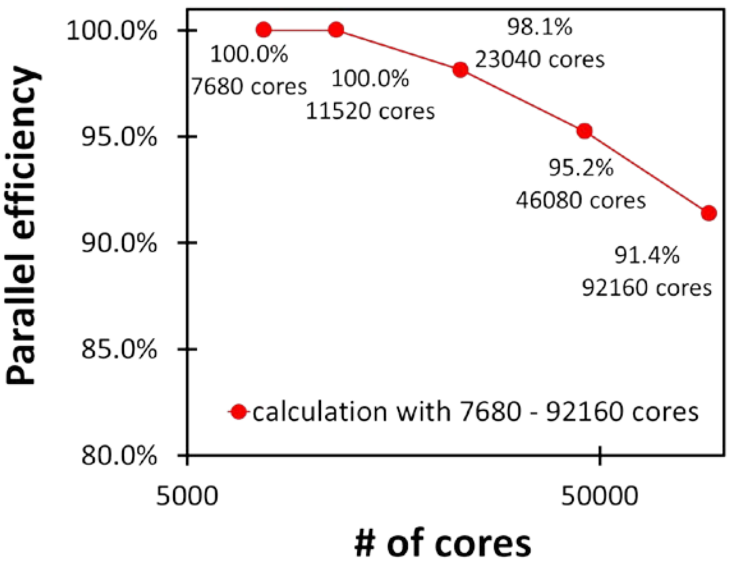

Computational time granted at K-computer for 2014 year.

- General use is admitted (4M node-hours)
- Use in strategic program is planned

We also have computational time at SuperMUC (LRZ, Germany)

Large-scale computation is indispensable

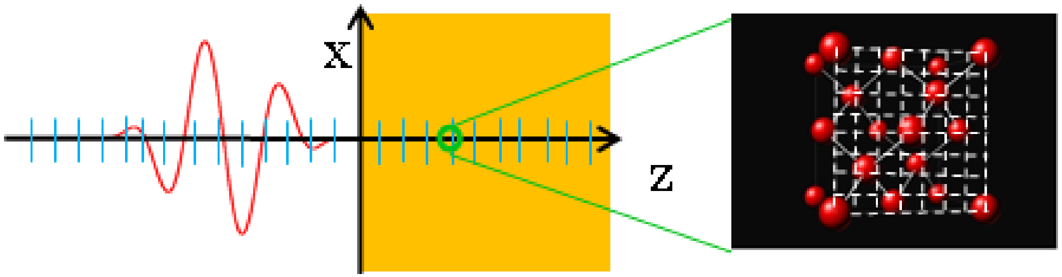

At present, 1-dim propagation (macroscopic grid)

Si, diamond:

1,000 cores, 10 hours

20,000 cores, 20 min (K-computer, Kobe)

SiO_2 (α-quartz)

30,000 cores, 2 hours

Oblique incidence, 2-dim

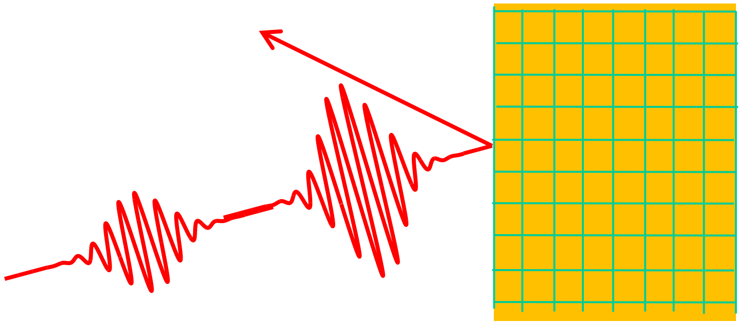

$\times 50$

3-dim

- Self focusing
- Circular polarization

A million of macro-grid points

$\times 1,000$

need to wait next generation supercomputers

International/Domestic Collaborations

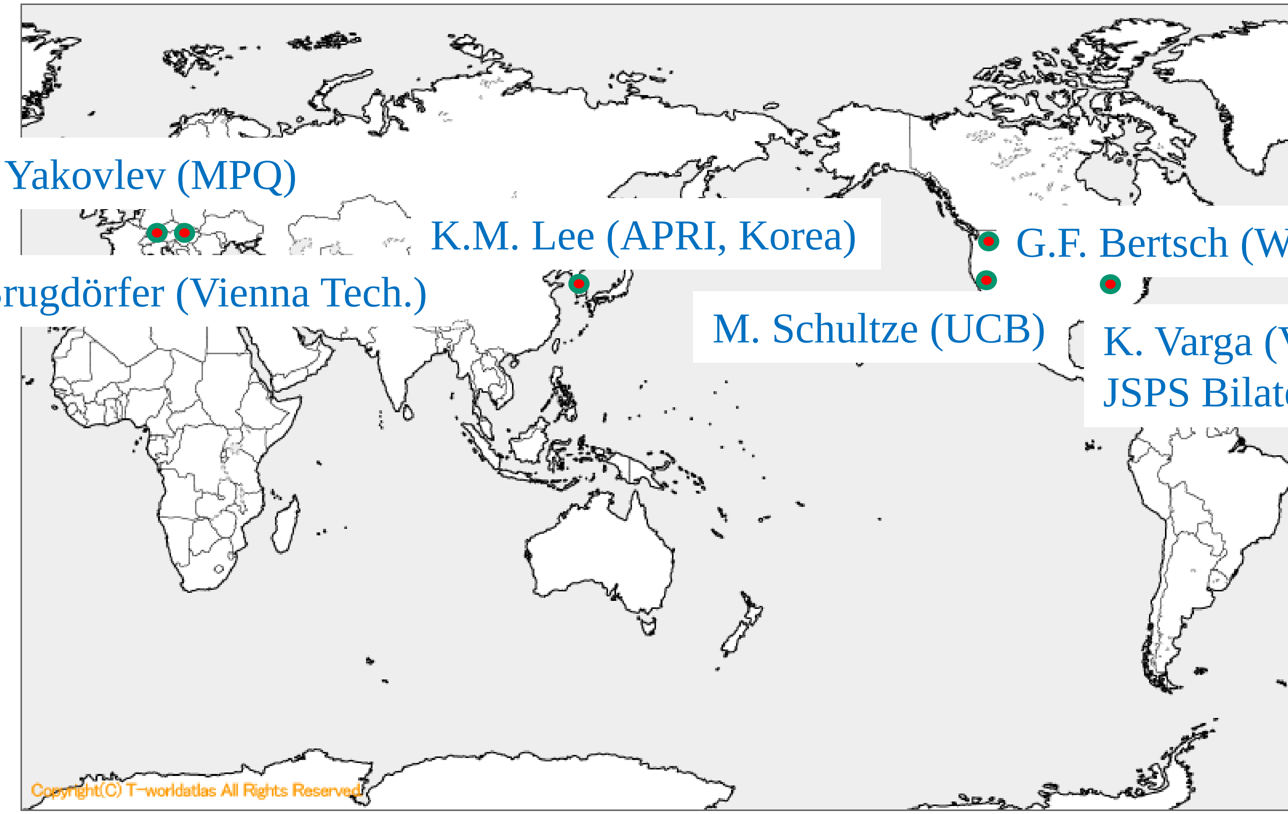

International/Domestic Collaborations

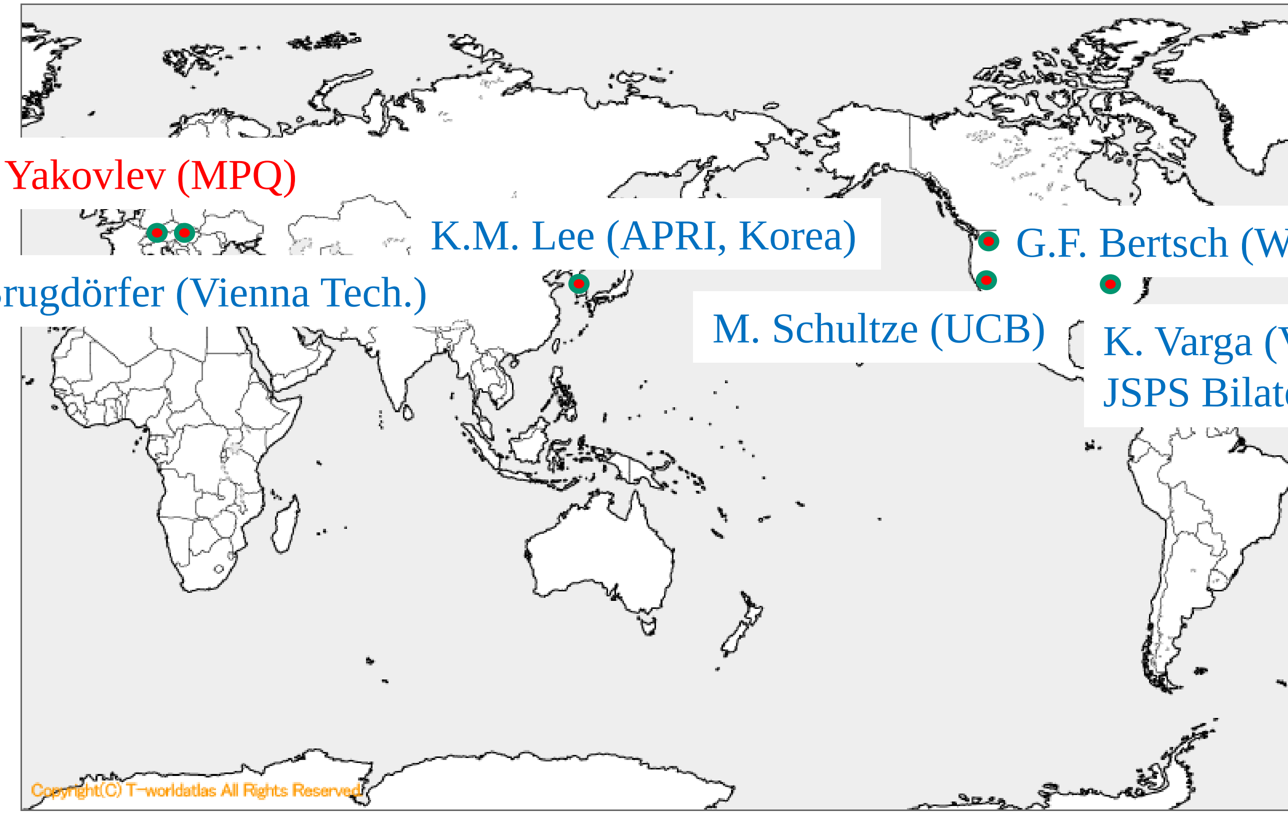

First-principles calculation of ablation depth of α-quartz (SiO_2)

$\hbar\omega = 1.55\text{eV}\ (\lambda = 800\text{nm}),\quad T = 10\text{fs}$

$E_{gap} = 6.5\,\text{eV (LDA)}$

Energy transfer from
Laser pulse to electrons

Ablation threshold intensity
$2.5\times10^{14}\ \text{W/cm}^2$
Ablation depth
: 100nm

Melting threshold intensity
$1\times10^{14}\ \text{W/cm}^2$
Melthing depth
600nm

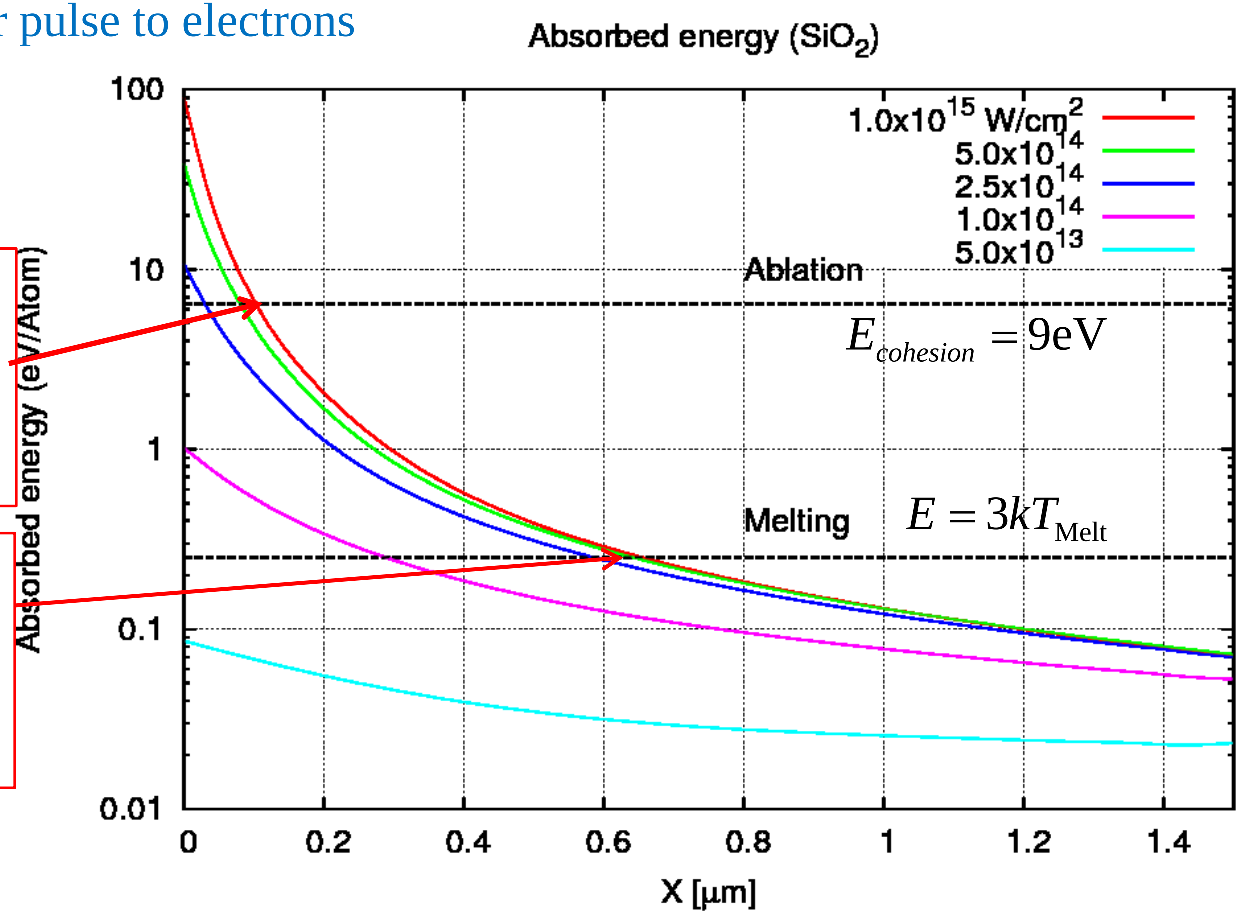

Typical computational time: 10,000 node-hours

HA-PACS: Multi-GPU calculation for hybrid functional

Hybrid functional provides a better performance for solids.
Calculation of the nonlocal exchange is the bottle neck.

$$\int d\vec{r}\,' \frac{e^2}{|\vec{r}-\vec{r}\,'|}\sum_{n'\vec{k}'} u_{n'\vec{k}'}(\vec{r})\, u^*_{n'\vec{k}'}(\vec{r}\,')\, w_{n\vec{k}}(\vec{r}\,') = -\sum_{n'\vec{k}'\vec{K}} u_{n'\vec{k}'}(\vec{r})\, e^{i\vec{K}\vec{r}} f^{\vec{K}}_{n'\vec{k}',n\vec{k}} \frac{4\pi e^2}{|\vec{K}+\vec{k}-\vec{k}'|^2}$$

$$f^{\vec{K}}_{n'\vec{k}',n\vec{k}} = \frac{1}{\Omega}\int_{\Omega} d\vec{r}\, e^{-i\vec{K}\vec{r}} u^*_{n'\vec{k}'}(\vec{r})\, w_{n\vec{k}}(\vec{r})$$

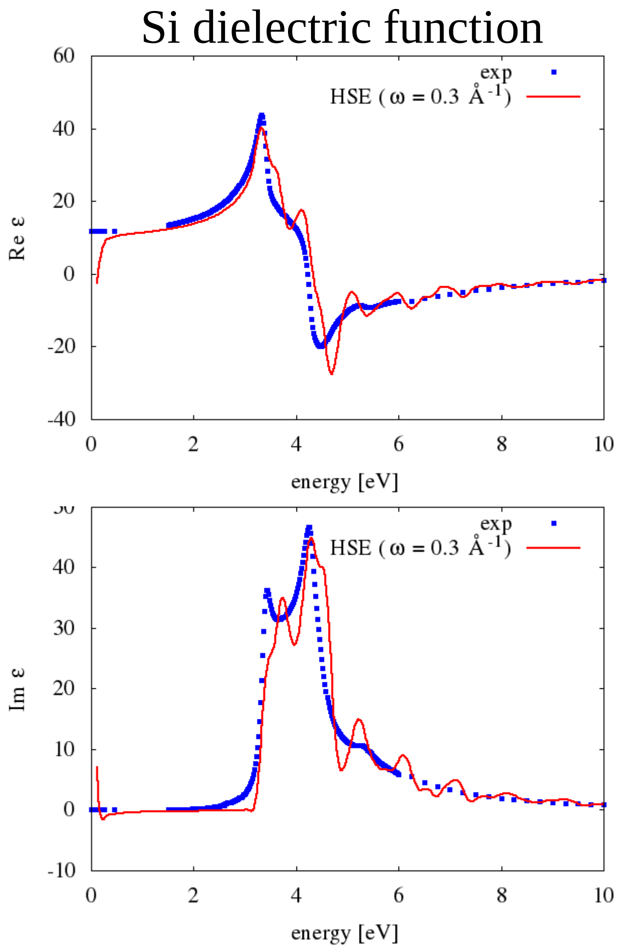

We accelerate it using HA-PACS multi-GPU machine:

Unit cell : cubic, 8 atoms/cell

k-points : 12^3 downsampled k-points : 4^3 spatial grid : 16^3

108 GPU(K2090), cuFFT $\Rightarrow$ 15 hours

Comparison with CPU (FFTW)

In one node, 4 GPUs is 4 times faster than 16 CPU cores

Code developments (ARTED):

Y. Shinohara (Ph.D, 2013, now JSPS fellowship, MPI-Halle)
S.A. Sato (M2, JSPS followship from April)
Y. Taniguchi (PD supported by the Center, developing GPU code)

Computer resources:

ISSP, Univ. of Tokyo
CCS, Univ. of Tsukuba
K-Computer (2014.4-, General project, Strategic program)

External financial support:

KAKENHI (Grants-in-Aid for Scientific Research, MEXT)
KIBAN(B) 2011-2015 ¥ 16M
Shin-gakujyutsu (Koubo) 2011-2012 ¥4M
Shin-gakujyutsu (Koubo) 2013-2014 ¥3M
Shin-gakujyutsu (Keikaku), under application
JSPS Bilateral International Collaboration between US-Japan
2013-2015, ¥ 5M